

## Dependence of Brillouin frequency shift on water absorption ratio in polymer optical fibers

Kazunari Minakawa,<sup>1,a)</sup> Kotaro Koike,<sup>2</sup> Neisei Hayashi,<sup>3</sup> Yasuhiro Koike,<sup>2</sup> Yosuke Mizuno,<sup>1</sup> and Kentaro Nakamura<sup>1,a)</sup>

<sup>1</sup>Laboratory for Future Interdisciplinary Research of Science and Technology, Tokyo Institute of Technology, 4259 Nagatsuta-cho, Midori-ku, Yokohama 226-8503, Japan

<sup>2</sup>Keio Photonics Research Institute, Keio University, 7-1 Shinkawasaki, Saiwai-ku, Kawasaki 212-0032, Japan

<sup>3</sup>Research Center for Advanced Science and Technology, The University of Tokyo, 4-6-1, Komaba, Meguro-ku, Tokyo 153-8904, Japan

(Received 29 March 2016; accepted 24 May 2016; published online 9 June 2016)

We studied the dependence of the Brillouin frequency shift (BFS) on the water-absorption ratio in poly(methyl methacrylate)-based polymer optical fibers (POFs) to clarify the effect of the humidity on POF-based Brillouin sensors. The BFS, deduced indirectly using an ultrasonic pulse-echo technique, decreased monotonically as the water absorption ratio increased, mainly because of the decrease in the Young's modulus. For the same water absorption ratio, the BFS change was larger at a higher temperature. The maximal BFS changes (absolute values) at 40, 60, and 80 °C were 158, 285, and 510 MHz, respectively (corresponding to the temperature changes of ~9 °C, ~16 °C, and ~30 °C). Thus, some countermeasure against the humidity is indispensable in implementing strain/temperature sensors based on Brillouin scattering in POFs, especially at a higher temperature. On the other hand, Brillouin-based distributed humidity sensors might be developed by exploiting the BFS dependence on water absorption in POFs. *Published by AIP Publishing.*

[<http://dx.doi.org/10.1063/1.4953388>]

### I. INTRODUCTION

Distributed strain/temperature sensing techniques have become increasingly important in a variety of application fields, including structural health monitoring and thermal management. Among them, strain/temperature sensing based on Brillouin scattering in optical fibers has attracted significant attention because it offers completely distributed sensing with high stability. Sensor heads of conventional Brillouin sensors are made of glass optical fibers (GOFs), which cannot withstand strains exceeding ~3%.<sup>1-9</sup> To improve the measurable strain limit, Brillouin sensors based on polymer optical fibers (POFs) have been extensively studied,<sup>10-16</sup> because they generally have high flexibility and can withstand significantly larger strains exceeding ~50%.<sup>17,18</sup>

To date, some of the fundamental properties of Brillouin scattering in POFs have been investigated, such as the Brillouin gain coefficient, the Brillouin threshold power, the Brillouin frequency shift (BFS), and its strain and temperature dependences.<sup>10-16,19-23</sup> The POF-based Brillouin sensing of strain and temperature distributions has also been demonstrated.<sup>14-16</sup> However, no reports have been provided on the effect of the humidity on the Brillouin properties of POFs. In standard silica GOFs, as reported, the BFS measured at 1500 nm increases by 0.3 MHz when the relative humidity is increased from 60% to 98%,<sup>24</sup> corresponding to a strain change of ~6.6 με<sup>1</sup> or a temperature change of ~0.3 °C.<sup>2,24</sup> This result indicates that the accuracy of Brillouin sensing is deteriorated by the ambient humidity. As polymers absorb larger amount of water,<sup>25</sup> the accuracy of

POF-based Brillouin sensors is also expected to be lowered by the humidity. Thus, it is of paramount importance to reveal the effect of water absorption on the Brillouin properties of POFs.

In this work, we evaluate the BFS dependence on the water absorption ratio in poly(methyl methacrylate)-based (PMMA-) POFs, which are most widely used for POF-based sensing and are reported as potentially applicable to Brillouin sensors.<sup>21</sup> The BFS decreased monotonically as the water absorption ratio increased. For the same water absorption ratio, the BFS change increased with the temperature. The maximal BFS changes (absolute values) caused by the water absorption at 40, 60, and 80 °C were 158, 285, and 510 MHz, respectively (corresponding to temperature changes of ~9 °C, ~16 °C, and ~30 °C).<sup>21</sup> Therefore, some preventive steps should be taken to mitigate the influence of the humidity and to develop accurate strain/temperature sensors based on Brillouin scattering in POFs.

### II. PRINCIPLE

Light transmitted through an optical fiber interacts with acoustic phonons in the core and is backscattered with a frequency downshift of several gigahertz. This phenomenon is known as Brillouin scattering, and the extent of the frequency downshift is termed the BFS.<sup>26</sup> The BFS can be expressed by<sup>1,26,27</sup>

$$BFS = \frac{2nv_a}{\lambda_p} = \frac{2n}{\lambda_p} \sqrt{\frac{1-\sigma}{(1-2\sigma)(1+\sigma)}} \frac{E}{\rho}, \quad (1)$$

where  $n$  is the refractive index,  $v_a$  is the acoustic velocity,  $\sigma$  is the Poisson's ratio,  $E$  is the Young's modulus, and  $\rho$  is the

<sup>a)</sup>Authors to whom correspondence should be addressed. Electronic addresses: kminakawa@sonic.pi.titech.ac.jp and knakamura@sonic.pi.titech.ac.jp

density of the fiber core;  $\lambda_p$  is the wavelength of the incident light. Since  $n$ ,  $\sigma$ ,  $E$ , and  $\rho$  depend on the fiber strain and the ambient temperature,<sup>28–36</sup> the BFS has the strain/temperature dependence.<sup>1,2</sup> Thus, by measuring the BFS, the strain- or temperature-related information, which is the foundation of Brillouin-based fiber-optic sensing of strain and temperature, can be derived.<sup>26</sup>

### III. METHODS

The direct observation of Brillouin scattering in PMMA-POFs is difficult because the low-loss window of the fibers is in the visible range, in which some of the optical devices required for fiber-optic Brillouin measurements are not available (note that Brillouin scattering has been observed at visible wavelength in bulk materials).<sup>37–39</sup> Therefore, we indirectly calculated the BFS dependence on the water-absorption ratio. Using a PMMA bulk sample (the Brillouin properties of PMMA-POFs with relatively large core diameters are reported to be almost the same as those of PMMA bulk samples),<sup>40</sup> we measured the acoustic-velocity change caused by water absorption, and then calculated the BFS dependence on the water absorption ratio using Eq. (1).

#### A. Preparation of the PMMA bulk sample

We prepared the PMMA bulk sample by free-radical polymerization. Methyl methacrylate (MMA) and di-tert-butyl peroxide (DTBP; used as an initiator) were purchased from Sigma Aldrich. The monomer was distilled using a spinning band column, and DTBP was used as received. The monomer mixture containing the initiator was transferred into a glass ampoule and subjected to repeated freeze-pump-thaw cycles. The ampoule was then flame-sealed in vacuum. The polymerization was conducted at 90 °C for 19 h and subsequently at 110 °C for 27 h to allow for complete polymerization of the monomers. After the polymerization, we measured the refractive index and the glass transition temperature ( $T_g$ ).

The refractive index was measured using a prism coupler with an accuracy of  $\pm 0.0005$  at room temperature. The probe wavelengths were 532.0, 632.8, 839.0, and 1544 nm. The measured values were fitted to the three-term Cauchy's equation.<sup>41</sup> Considering that PMMA-POFs will be used as Brillouin sensors at  $\sim 650$  nm (low-loss window),<sup>42</sup> the refractive index at this wavelength was used (calculated to be 1.489).

The  $T_g$  value was determined using a differential scanning calorimeter at a scan rate of 10 °C/min under dry nitrogen. To avoid the measurement error caused by enthalpy relaxation, the  $T_g$  measurement was performed during the second heating scan at the midpoint of the heat capacity transition between the upper and lower points of the deviation from the extrapolated rubber and glass lines. The  $T_g$  value was then estimated to be 124 °C.

#### B. Estimation of the BFS dependence on the water-absorption ratio

We cut the PMMA bulk (polymerized as described in Section III A) into a 1.50 mm thick cylindrical sample. The

sample was dried and immersed in pure water at a constant temperature to measure the water absorption ratio as a function of the immersion time. The water absorption ratio was defined as the increase in weight as a percentage of the original weight.

After the measurement, the sample was dried again, and we investigated its BFS with respect to the immersion time using an ultrasonic pulse-echo technique.<sup>40</sup> First, as shown in Fig. 1, the sample was placed in degassed pure water of the same temperature as was used during the water-absorption ratio measurement. Next, ultrasonic pulses with a central frequency of 20 MHz were delivered to the sample by an ultrasonic transducer, and the reflected signals from the top and bottom of the sample were recorded using the same transducer. By measuring the temporal delay  $\Delta t$  between the two reflected waves using an oscilloscope, we calculated the acoustic velocity  $v_a$  in the PMMA sample as

$$v_a = \frac{2l}{\Delta t}, \quad (2)$$

where  $l$  is the sample thickness ( $=1.50$  mm). Next, we calculated the BFS at  $\lambda_p = 650$  nm by substituting the acoustic velocity and the refractive index  $n$  into Eq. (1). Here, as  $n$  decreased only by  $\sim 0.1\%$  (corresponding to  $\sim 0.1\%$  decrease in the BFS), we assumed the  $n$  value to be constant ( $=1.489$ ) during the measurement. These procedures were repeated while the sample was immersed for 72–96 h, yielding the BFS dependence on the immersion time.

Finally, by combining the aforementioned two measurement results (water absorption ratio vs. immersion time; BFS vs. immersion time), we derived the BFS dependence on the water absorption ratio.

### IV. EXPERIMENTAL RESULTS

Figure 2(a) shows the water-absorption ratio at three different temperatures (40, 60, and 80 °C, respectively) plotted with respect to the water-immersion time. This temperature range was set by considering that glass-rubber phase transitions generally occur at temperatures lower than  $T_g$  by several dozen degrees<sup>43,44</sup> and that the transition to the rubbery state caused the physical deformation of the sample, making the sample thickness difficult to measure accurately. The measured data were fitted using the following equation:<sup>45</sup>

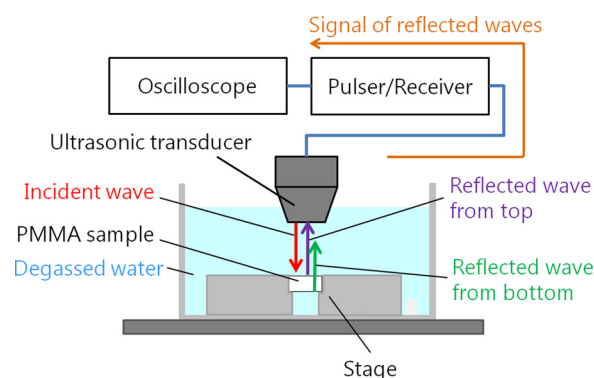


FIG. 1. Experimental setup for the estimation of the BFS in the PMMA sample.

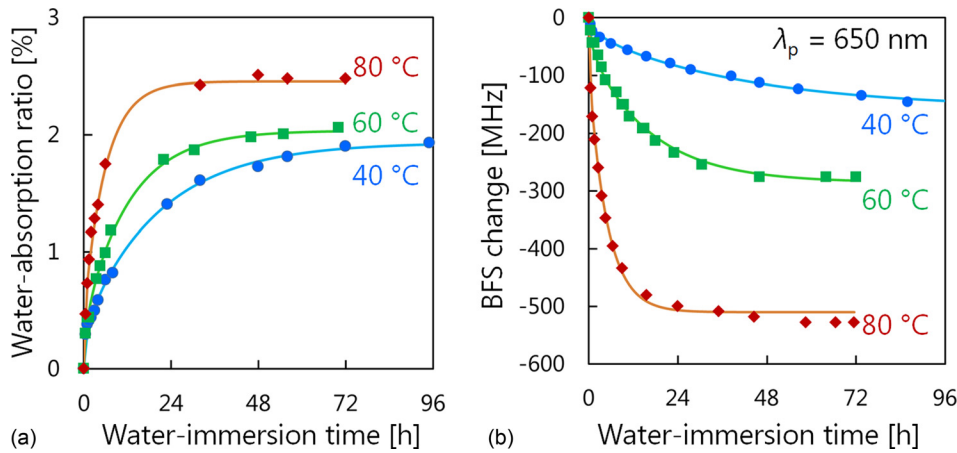


FIG. 2. (a) Water-absorption ratio and (b) BFS change vs. water-immersion time for the PMMA sample. The data were fitted using Eq. (3).

$$c(t) = c_s - \frac{8c_s}{\pi^2} \sum_{k=1}^{20} \frac{1}{(2k-1)^2} \exp\left(-\frac{(2k-1)^2 D \pi^2 t}{l^2}\right), \quad (3)$$

where  $c(t)$  is the water-absorption ratio at immersion time  $t$ ,  $c_s$  is the saturated water-absorption ratio, and  $D$  is the diffusion coefficient of the bulk sample. The water-absorption ratio increased with the water-immersion time. The change was most pronounced at  $<24$  h and nearly leveled off at  $>96$  h. As the temperature increased, the saturation time shortened and the water-absorption ratio at the steady state increased. The saturated water absorption ratios at 40, 60, and 80 °C were 1.9, 2.0, and 2.5%, respectively.

Figure 2(b) shows the BFS dependence on the immersion time at 650 nm at 40, 60, and 80 °C. The BFS changes were observed after the sample was immersed for  $\sim 40$  s (note that the sample absorbs almost no water at the immersion time of  $\sim 40$  s) to exclude the BFS change caused by heating.<sup>21</sup> We fitted the obtained BFS values using Eq. (3), considering that the BFS change will roughly follow the change in the water-absorption ratio (this assumption appears to be valid because the temporal variations of the BFS changes in Fig. 2(b) showed similar trends to those in Fig. 2(a)). When the immersion time increased, the BFS decreased, opposite to GOFs.<sup>24</sup> The BFS changes (absolute values) at the steady state were 158, 285, and 510 MHz corresponding to temperature changes of  $\sim 9$ ,  $\sim 16$ , and  $\sim 30$  °C, respectively.<sup>21</sup>

By combining the observations in Figs. 2(a) and 2(b), we calculated the BFS dependence on the water-absorption ratio (Fig. 3). The BFS monotonically decreased as the water-absorption ratio increased. For the same water-absorption ratio, the BFS change (absolute value) was larger when the temperature was higher. At  $<1.5\%$ , the BFS dependence on the water-absorption ratio was almost linear with the coefficients of approximately  $-47$ ,  $-124$ , and  $-225$  MHz at 40, 60, and 80 °C, respectively.

These results indicate that measurements should be taken to assuage the effect of the humidity to maintain the accuracy of strain/temperature sensing based on Brillouin scattering in PMMA-POFs, especially at a higher temperature. One such method is based on coating POFs with waterproof materials such as polypropylene<sup>46</sup> and polyethylene.<sup>47</sup> The use of perfluorinated graded-index POFs, which are

reported to absorb no quantifiable water,<sup>48</sup> is also a promising solution. However, this disadvantage becomes an advantage for humidity sensing. For example, using the BFS dependence on the humidity in POFs, distributed Brillouin humidity sensing might be implemented by exploiting conventional time-,<sup>3,4,7</sup> frequency-,<sup>8</sup> and correlation-domain techniques.<sup>5,6</sup>

## V. DISCUSSION

Here, we discuss which of the four parameters (refractive index  $n$ , the Poisson's ratio  $\sigma$ , the Young's modulus  $E$ , and the density  $\rho$ ; see Eq. (1)) most dominantly causes the BFS change when the PMMA sample is immersed in water. To clarify this, we compared their values before and after saturated water absorption at 60 °C.

When the water absorption ratio is saturated, the refractive index  $n$  decreased by  $\sim 0.1\%$ , which corresponds to  $\sim 0.1\%$  decrease in the BFS, as described in Sec. III A. Likewise, the density  $\rho$ , measured using the water displacement method with a density determination kit (AD-1653, A&D), decreased by  $\sim 0.3\%$ , which corresponds to  $\sim 0.2\%$  increase in the BFS. The Poisson's ratio  $\sigma$  and the Young's modulus  $E$  of the PMMA sample were measured using a compression tester described in Fig. 4. We attached two

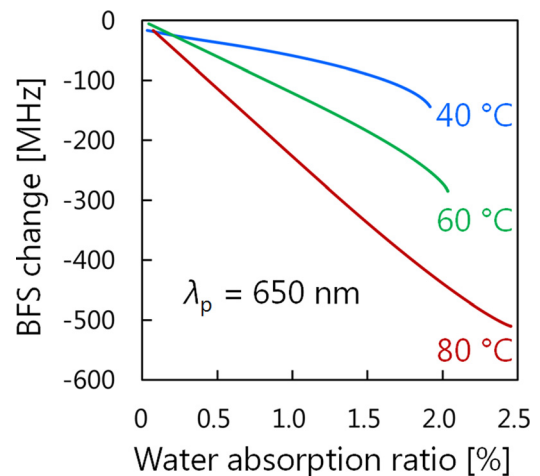


FIG. 3. BFS dependence on the water absorption ratio for PMMA; the dependence was calculated using the fitted curves presented in Figs. 2(a) and 2(b).

strain gauges to measure the vertical strain  $\varepsilon_v$  and lateral strain  $\varepsilon_l$ , and then calculated  $\sigma$  using the following equation:<sup>49</sup>

$$\sigma = -\frac{\varepsilon_l}{\varepsilon_v}. \quad (4)$$

On the other hand, the  $E$  value was calculated as the slope of the stress-strain curve in the elastic region.<sup>49</sup> When the PMMA sample absorbed water, the  $E$  value decreased by  $\sim 11\%$ , which corresponds to  $\sim 6\%$  decrease in the BFS, whereas the  $\sigma$  value was 0.40 and showed no dependence on the water-absorption ratio in this measurement (with a maximal measurement error of 0.01). Although there should be a correlation between  $\sigma$  and  $E$ ,<sup>49,50</sup> the change rate of  $\sigma$  is usually negligibly small compared to that of  $E$ . Thus, we deduce that the reduction in the Young's modulus is the major cause for the BFS reduction by water absorption.

## VI. CONCLUSION

We investigated the BFS dependence on the water absorption ratio in PMMA to clarify the effect of the humidity on POF-based Brillouin sensors. The BFS decreased monotonically as the water-absorption ratio increased, mainly because of the decrease in the Young's modulus. For the same water-absorption ratio, the BFS change (absolute value) became larger with the increase in the temperature. The maximal BFS changes (absolute values) caused by the water absorption at 40, 60, and 80 °C were 158, 285, and 510 MHz, respectively (corresponding to temperature changes of  $\sim 9^\circ\text{C}$ ,  $\sim 16^\circ\text{C}$ , and  $\sim 30^\circ\text{C}$ ).<sup>21</sup> The dependences were almost linear when the water-absorption ratio was  $< 1.5\%$ . The coefficients at 40, 60, and 80 °C were approximately  $-47$ ,  $-124$ , and  $-225$  MHz, respectively. Thus, to develop accurate strain/temperature sensors based on Brillouin scattering in PMMA-POFs, especially for using them at a higher temperature, we need to take some actions to reduce the effect of the humidity, either by coating PMMA-POFs with waterproof materials or by using special POFs with almost no water absorption. However, for humidity sensing, the monotonic BFS dependence on the humidity in PMMA-POFs becomes an advantage. Along with the

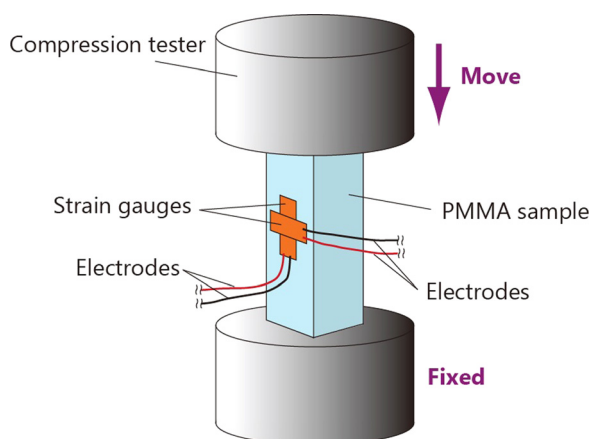


FIG. 4. Compression tester for measuring the Poisson's ratio and the Young's modulus in the PMMA sample (dimension:  $6.0 \times 6.0 \times 20.0 \text{ mm}^3$ ).

strain and temperature, the humidity can be measured by distributed Brillouin sensing. We hope that the results described in this work will be an important step towards future development of next-generation Brillouin sensors.

## ACKNOWLEDGMENTS

The authors are indebted to Masaki Tahara, Hideki Hosoda, Minoru Kuribayashi Kurosawa, Wei Qiu, and Jiang Wu, Tokyo Institute of Technology, Japan, for their experimental assistance. They also acknowledge the staff of the Technical Department, Tokyo Institute of Technology, Japan, for fabricating the stage used in the experiments. This work was supported by the JSPS KAKENHI Grant Numbers 25709032, 26630180, 25007652, and 15J11445, and by research grants from the Iwatani Naoji Foundation, the SCAT Foundation, and the Konica Minolta Science and Technology Foundation.

<sup>1</sup>T. Horiguchi, T. Kurashima, and M. Tateda, *IEEE Photonics Technol. Lett.* **1**, 107 (1989).

<sup>2</sup>T. Kurashima, T. Horiguchi, and M. Tateda, *Appl. Opt.* **29**, 2219 (1990).

<sup>3</sup>T. Horiguchi and M. Tateda, *J. Lightwave Technol.* **7**, 1170 (1989).

<sup>4</sup>Y. Dong, D. Ba, T. Jiang, D. Zhou, H. Zhang, C. Zhu, Z. Lu, H. Li, L. Chen, and X. Bao, *IEEE Photonics J.* **5**, 2600407 (2013).

<sup>5</sup>K. Hotate and T. Hasegawa, *IEICE Trans. Electron.* **E83-C**, 405 (2000).

<sup>6</sup>Y. Mizuno, W. Zou, Z. He, and K. Hotate, *Opt. Express* **16**, 12148 (2008).

<sup>7</sup>T. Kurashima, T. Horiguchi, H. Izumita, S. Furukawa, and Y. Koyamada, *IEICE Trans. Commun.* **E76-B**, 382 (1993).

<sup>8</sup>D. Garus, K. Krebber, F. Schliep, and T. Gogolla, *Opt. Lett.* **21**, 1402 (1996).

<sup>9</sup>Y. Dong, L. Teng, P. Tong, T. Jiang, H. Zhang, T. Zhu, L. Chen, X. Bao, and Z. Lu, *Opt. Lett.* **40**, 5003 (2015).

<sup>10</sup>Y. Mizuno and K. Nakamura, *Appl. Phys. Lett.* **97**, 021103 (2010).

<sup>11</sup>Y. Mizuno and K. Nakamura, *Opt. Lett.* **35**, 3985 (2010).

<sup>12</sup>K. Minakawa, N. Hayashi, Y. Shinohara, M. Tahara, H. Hosoda, Y. Mizuno, and K. Nakamura, *Jpn. J. Appl. Phys., Part 1* **53**, 042502 (2014).

<sup>13</sup>N. Hayashi, Y. Mizuno, and K. Nakamura, *Opt. Express* **20**, 21101 (2012).

<sup>14</sup>A. Minardo, R. Bernini, and L. Zeni, *IEEE Photon. Technol. Lett.* **26**, 387 (2014).

<sup>15</sup>Y. Dong, P. Xu, H. Zhang, Z. Lu, L. Chen, and X. Bao, *Opt. Express* **22**, 26510 (2014).

<sup>16</sup>N. Hayashi, Y. Mizuno, and K. Nakamura, *J. Lightwave Technol.* **32**, 3999 (2014).

<sup>17</sup>M. G. Kuzzyk, *Polymer Fiber Optics: Materials, Physics, and Applications* (CRC Press, 2006).

<sup>18</sup>H. Ujihara, N. Hayashi, M. Tabaru, Y. Mizuno, and K. Nakamura, *IEICE Electron. Express* **11**, 20140707 (2014).

<sup>19</sup>N. Hayashi, K. Minakawa, Y. Mizuno, and K. Nakamura, *Appl. Phys. Lett.* **105**, 091113 (2014).

<sup>20</sup>K. Minakawa, K. Koike, N. Hayashi, Y. Koike, Y. Mizuno, and K. Nakamura, *IEICE Electron. Express* **11**, 20140285 (2014).

<sup>21</sup>N. Hayashi, Y. Mizuno, D. Koyama, and K. Nakamura, *Appl. Phys. Express* **5**, 032502 (2012).

<sup>22</sup>K. Minakawa, N. Hayashi, Y. Mizuno, and K. Nakamura, *Appl. Phys. Express* **6**, 052501 (2013).

<sup>23</sup>K. Minakawa, K. Koike, Q. Du, N. Hayashi, Y. Koike, Y. Mizuno, and K. Nakamura, *J. Appl. Phys.* **117**, 144505 (2015).

<sup>24</sup>C. Galindez, F. J. Madruga, and J. M. Lopez-Higuera, *IEEE Photonics Technol. Lett.* **20**, 1959 (2008).

<sup>25</sup>M. Unemori, Y. Matsuya, S. Matsuya, A. Akashi, and A. Akamine, *Biomaterials* **24**, 1381 (2003).

<sup>26</sup>G. P. Agrawal, *Nonlinear Fiber Optics* (Academic Press, San Diego, 1995).

<sup>27</sup>K. F. Graff, *Wave Motion in Elastic Solids* (Dover Publications, New York, 1975).

<sup>28</sup>G. B. Hocker, *Appl. Opt.* **18**, 1445 (1979).

<sup>29</sup>R. M. Waxler, D. Horowitz, and A. Feldman, *Appl. Opt.* **18**, 101 (1979).

<sup>30</sup>K. Suito, M. Miyoshi, T. Sasakura, and H. Fujisawa, *High-Pressure Research: Application to Earth and Planetary Sciences* (Terra Scientific

- Publishing Company and American Geophysical Union, Tokyo and Washington DC, 1992), pp. 219–225.
- <sup>31</sup>C. Z. Tan and J. Arndt, *J. Phys. Chem. Solids* **61**, 1315 (2000).
- <sup>32</sup>J. M. Cariou, J. Dugas, L. Martin, and P. Michel, *Appl. Opt.* **25**, 334 (1986).
- <sup>33</sup>R. Kono, *J. Phys. Soc. Jpn.* **15**, 718 (1960).
- <sup>34</sup>J. W. Marx and J. M. Sivertsen, *J. Appl. Phys.* **24**, 81 (1953).
- <sup>35</sup>M. Fukuhara and A. Sampei, *J. Polym. Sci. Part B: Polym. Phys.* **33**, 1847 (1995).
- <sup>36</sup>J. J. Curro and R. J. Roe, *Polymer* **25**, 1424 (1984).
- <sup>37</sup>J. A. Forrest, K. Dalnoki-Veress, and J. R. Dutcher, *Phys. Rev. E* **58**, 6109 (1998).
- <sup>38</sup>G. Floudas, G. Fytas, and I. Alig, *Polymer* **32**, 2307 (1991).
- <sup>39</sup>J. R. Sandercock, *Phys. Rev. Lett.* **28**, 237 (1972).
- <sup>40</sup>N. Hayashi, Y. Mizuno, D. Koyama, and K. Nakamura, *Appl. Phys. Express* **4**, 102501 (2011).
- <sup>41</sup>A. L. Cauchy, *Mémoire sur la Dispersion de la Lumière* (J. G. Calve, Prague, 1836).
- <sup>42</sup>T. Kaino, K. Jinguji, and S. Nara, *Appl. Phys. Lett.* **42**, 567 (1983).
- <sup>43</sup>S. D. Clas, C. R. Dalton, and B. C. Hancock, *Pharm. Sci. Technol. Today* **2**, 311 (1999).
- <sup>44</sup>L. S. A. Smith and V. Schmitz, *Polymer* **29**, 1871 (1988).
- <sup>45</sup>UNE-EN ISO 62: 2008, Plastics—Determination of water absorption.
- <sup>46</sup>M. Tajvidi, S. K. Najafi, and N. Moteei, *J. Appl. Polym. Sci.* **99**, 2199 (2006).
- <sup>47</sup>K. B. Adhikary, S. Pang, and M. P. Staiger, *Composites Part B* **39**, 807 (2008).
- <sup>48</sup>S. Ando, T. Matsuura, and S. Sasaki, *CHEMTECH* **24**, 20 (1994).
- <sup>49</sup>L. H. Sperling, *Introduction to Physical Polymer Science* (John Wiley & Sons, Hoboken, 2005).
- <sup>50</sup>A. F. Yee and M. T. Takemori, *J. Polym. Sci.: Polym. Phys. Ed.* **20**, 205 (1982).